Hyperelasticity Modeling for Incompressible Passive Biological Tissues

Grégory Chagnon, Jacques Ohayon, Jean-Louis Martiel, Denis Favier

Hyperelasticity Modeling for Incompressible Passive Biological Tissues

G. Chagnon, J. Ohayon, J. L. Martiel, D. Favier

Université Grenoble-Alpes, TIMC-IMAG, F-38000 Grenoble, France.

CNRS, TIMC-IMAG, F-38000Grenoble, France

Abstract

Soft tissues are mainly composed of organised biological media giving them an anisotropic mechanical behavior. Soft tissues also have the ability to undergo large elastic reversible deformations. Many constitutive models were developed to describe these phenomena. In this chapter, we discuss several varying models and their constitutive equations which are defined by means of strain components or strain invariants. The notion of tangent moduli will be plotted for two well-known constitutive equations, and, we will illustrate how to implement explicitly a structural kinematics constraint in a constitutive law to derive the resulting Cauchy stress tensor.

Keywords: Hyperelasticity, Anisotropy, Kinematics constraint, Lagrange multiplier, Strain-Energy density functions

1. Introduction

In the last decades there has been a significant growth in interest to characterize the passive anisotropic mechanical properties of soft incompressible biological tissues based on nonlinear continuum theory. Such constitutive approach is suitable to describe a wide variety of physical material behaviors in which the strain may be large [1, 2, 3, 4, 5]

Biological tissues are heterogeneous composite materials made of different media as epithelial, connective, muscular, neuronal... [6]. In these composite materials, the distributions of the internal constituents are assumed to be locally uniform on the continuum scale. These tissues are often regarded as oriented cells surrounded by an extra cellular matrix, the whole behaving as anisotropic continuum media reinforced by different families of fibres of distinct orientations. The proportion of matrix and fibres, as their orientations, depend on the type of soft tissues (artery, skin, cornea, muscle). All these materials present a complex mechanical behavior [7, 8],and can often support large reversible deformations and strains. They can also present some other physical phenomena as viscoelasticity [9, 10], stress softening [11, 12], strain hardening [13].

It is the aim of constitutive theories to develop mathematical models reproducing the real behavior of biological tissues. Based on the nonlinear continuum mechanics theory, the anisotropic constitutive law of the soft tissue can be derived from a strain-energy density function (SEDF) W, which is defined per unit of reference volume. Such SEDF is expressed as a function of the deformation gradient ($\mathbf{F}$) or the Green-Lagrange strain tensors ($\mathbf{E}$)) (i.e. $W = W(\mathbf{F})) = W(\mathbf{E}))$).

Email address: gregory.chagnon@imag.fr (G. Chagnon)

Two main formulations are used in the literature to express a SEDF. The first is based on the use of the Green-Lagrange strain tensor components, while in the second is expressed in term of strain invariants. For these two approaches, many constitutive models have been proposed in literature [14]. And although a thorough review and classification of all models is beyond the scope of this chapter, we will present and highlight some specific and pioneer models.

In this chapter, we will first introduce the notion of hyperelasticity. We will then present several well-known pioneer constitutive models using the two SEDF formulations. Additionally, we will exemplify how a constitutive stress-strain law can account for a kinematics constraint. And finally, by using two well-known SEDFs we will discuss the changes of the tangent elasticity moduli during uniaxial extension tests. The relationships between the parameter of these two SEDFs and the linear elasticity constant in small deformations will also be provided. Such relationships could be used to improve the identification method that needs to be conducted to quantify the material constants.

2. Mechanical formulation

2.1. Description of the deformation

The deformation of soft tissues is often described by means of the right and left Cauchy-Green tensors defined as: $\mathbf{C} = \mathbf{F}^T\mathbf{F}$ and $\mathbf{B} = \mathbf{F}\mathbf{F}^T$, where $\mathbf{F}$ is the deformation gradient. The principle components of the right or left Cauchy-Green tensors are λ_i^2 with $i = 1..3$; λ_i are called the stretches. The logarithmic strains are simply expressed as $\epsilon_i = \ln(\lambda_i)$ in the principal basis. The Green-Lagrange strain tensor is directly defined in function of the right strain tensor by $\mathbf{E} = (\mathbf{C} - \mathbf{I})/2$, where $\mathbf{I}$ is the identity tensor, and its components are noted E_{ij} with $i, j = 1...3$. As the strain tensor components values depend on the basis in which they are written, some use the stain invariants to express them. These invariant are defined for isotropic media as:

$$I_1 = \mathrm{tr}(\mathbf{C}),\ \ I_2 = \frac{1}{2}\left[\mathrm{tr}(\mathbf{C})^2 - \mathrm{tr}(\mathbf{C}^2)\right],\ \text{ and }\ I_3 = \det(\mathbf{C}) \tag{1}$$

where "tr" is the trace operator, and "det" the determinant operator. It is to note that for incompressible materials $I_3 = 1$.

To describe the mechanical properties of a reinforced fibrous material, it is necessary to define fibre orientations. The fibres families are numbered i from 1 to q. An unit vector $\mathbf{N}^{(i)}$ is introduced to describe the initial orientation of the i^{th} fibre. An initial orientation tensor is defined as $\mathbf{A}^{(i)} = \mathbf{N}^{(i)} \otimes \mathbf{N}^{(i)}$. During deformation process, each material direction is transformed into $\mathbf{n}^{(i)} = \mathbf{F}\mathbf{N}^{(i)}$, it represents the orientation of the fibre in the current state but $\mathbf{n}^{(i)}$ is not a unit vector.

The introduction of such directions leads to the definition of additional invariants relied to each direction. The invariant formulation of anisotropic constitutive equations is based on the concept of structural tensors [15, 16, 17]. The invariants I_4 and I_5 can be defined for one direction i as:

$$I_4^{(i)} = \mathrm{tr}(\mathbf{C}\mathbf{A}^{(i)}) = \mathbf{N}^{(i)} \cdot \mathbf{C}\mathbf{N}^{(i)},\quad \text{and}\quad I_5^{(i)} = \mathrm{tr}(\mathbf{C}^2\mathbf{A}^{(i)}) = \mathbf{N}^{(i)} \cdot \mathbf{C}^2\mathbf{N}^{(i)}. \tag{2}$$

In the literature, in the case of two fibre directions (1) and (2), a notation I_4 and I_6 is often used for soft tissues [18] instead of $I_4^{(1)}$ and $I_4^{(2)}$ (or I_5 and I_7 instead of $I_5^{(1)}$ and $I_5^{(2)}$).

These invariants depend only on one direction but it is possible to take into account the interaction between the different directions, by introducing a coupling between directions (i) and (j) by means of two other invariants:

$$I_8^{(i,j)} = (\mathbf{N}^{(i)} \cdot \mathbf{N}^{(j)})(\mathbf{N}^{(i)} \cdot \mathbf{C}\mathbf{N}^{(j)}),\quad \text{and}\quad I_9^{(i,j)} = (\mathbf{N}^{(i)} \cdot \mathbf{N}^{(j)})^2. \tag{3}$$

$I_9^{(i,j)}$ does not depend on $\mathbf{C}$ and therefore does not affects the stress tensor components. Its values corresponds to the value of $I_8^{(i,j)}$ for $\mathbf{C} = \mathbf{I}$, i.e. for no deformation. It is to note that other invariants were also proposed in the literature [19, 20, 21] even if they are few used for the description of soft tissue mechanical behaviour.

2.2. Strain-stress relationships

Living tissues are often considered as incompressible, thus the equations are written in a pure incompressible framework, i.e. $I_3 = 1$. The second Piola-Kirchhoff stress tensor can be directly calculated by derivation of the strain energy function written in function of the whole invariants: $W(I_1, I_2, I_4^{(i)}, I_5^{(i)}, I_8^{(i,j)}, I_9^{(i,j)})$, with $i, j = 1..q$:

$$\mathbf{S} = 2\left[(W_{,1} + I_1 W_{,2})\mathbf{I} - W_{,2}\mathbf{C} + \sum_i^q W_{,4}^{(i)} \mathbf{N}^{(i)} \otimes \mathbf{N}^{(i)} + \sum_i^q W_{,5}^{(i)} \left(\mathbf{N}^{(i)} \otimes \mathbf{C}\mathbf{N}^{(i)} + \mathbf{N}^{(i)}\mathbf{C} \otimes \mathbf{N}^{(i)}\right) + \sum_{i \neq j} W_{,8}^{(i,j)} (\mathbf{N}^{(i)} \cdot \mathbf{N}^{(j)})(\mathbf{N}^{(i)} \otimes \mathbf{N}^{(j)} + \mathbf{N}^{(j)} \otimes \mathbf{N}^{(i)})\right] + p\mathbf{C}^{-1} \tag{4}$$

where $W_{,k} = \frac{\partial W}{\partial I_k}$, and p is the hydrostatic pressure. The Eulerian stresses, *i.e.*, the Cauchy stresses are directly obtained by the Push-forward operation [3]. To ensure that the stress is identically zero in the non-deformed configuration, it is required that for each fibre orientation:

$$\forall i \quad W_{,4}^{(i)} + 2W_{,5}^{(i)} = 0, \tag{5}$$

for zero deformation [22].

The use of these equations in a finite element codes imposes to use a quasi-incompressible framework with a decomposition into volumetric and isochoric parts of the energy density. Details about the elasticity tensors are given in [23, 24, 25, 26]. A particular attention should be focused on the choice of the volumetric function in order to avoid any non-physical response [27, 28, 29].

2.3. Stability

The strain energy density cannot be chosen without restriction, the strong ellipticity condition must be verified. For three-dimensional problems [30], the strong ellipticity was characterised for compressible isotropic materials [31], and for incompressible ones [32]. The generic condition to verify for the strain energy in the absence of body forces [33, 34, 35] can be written as:

$$\frac{1}{J} F_{pr} F_{qs} \frac{\partial^2 W}{\partial F_{ir} F_{js}} n_p n_q m_i m_j > 0 \text{ with } \mathbf{m} \neq \mathbf{0} \text{ and } \mathbf{n} \neq \mathbf{0}, \tag{6}$$

where $\mathbf{m}$ and $\mathbf{n}$ are arbitrary two non-zero vectors. Nevertheless, this condition is always difficult to verify. Thus, some proposed another way to tackle the strong ellipticity condition. It is known that polyconvexity implies ellipticity [36, 37, 38]. As a consequence, the polyconvexity in the sense of Ball [39, 40] is used, even if it is more restrictive than strong ellipticity.

3. Constitutive equations for soft biological tissues

Even if soft tissues are made of cells and fibres, when the quantity of fibres is weak or when their mechanical influence can be neglected, an isotropic modelling can be efficient. Most of isotropic constitutive equations were not developed for soft tissues but for rubber like materials and used for soft tissues, they are listed in [41, 42]. Nevertheless, soft tissues often present a larger strain hardening than rubber like materials. This implies to the development of specific constitutive equations, the clue for the constitutive equations is to present an important change of slope in the strain-stress curve for moderate deformations. This leads to the development of many constitutive equations with exponential form. In an isotropic point of view, Demiray et al [43] proposed:

$$W = \frac{c_1}{c_2}\left\{\exp\left[\frac{c_2}{2}(I_1-3)^2\right]-1\right\} \tag{7}$$

where c_1, c_2 are material parameters. Similar exponential forms can be proposed for the second invariant [44] but this invariant is very rarely used for soft tissues. Nevertheless, the use of isotropic approach is very limited, anisotropic modelling are necessary to capture the real behaviour of many soft tissues.

3.1. Introduction to anisotropy

The anisotropy of the tissues depends on the characteristics of its components i.e. fibres, matrix and the interaction between them. It exists some modelling that tend to describe the soft tissues from a statistical point of view. It relies on the study of the collagen network and it uses an upscaling method [45, 46]. A collagen molecule is defined by its length, its stiffness and its helical structure. Some studies come from approaches developed for rubber like material [47, 48, 49]. Unlike polymer chains in rubber which are uncorrelated nature, collagen chains in biological tissues have to be classified as correlated chains for a statistical point of view. It this way, different theories are considered to represent the chains, as for example wormlike chains with a slight varying curvature [50], or sinusoidal, zig-zag or circular helix representations [51, 52, 53]. This leads to the development of constitutive equations that need numerical tool for integration in space. A good use of these models necessitates specific experimental measures of the physiological properties of the soft tissues.

In this chapter, it is decided to focus more on phenomenological equations that are directly expressed by means of strain components or strain invariants. But the choice of the number of fibre directions depends on the morphology of the tissue. The easiest formulation is with one direction to represent transverse isotropic behaviour but in other cases, more directions are needed. For example, in the first modelling of arteries mechanical behaviour, two fibre directions were used [54], before being extended to four directions [55, 56] and to n directions [57] and used for example with eight directions for cerebral aneurysms [58]. The reinforced directions can also be used as equivalent mechanical behaviour without any physical meaning, this means that model directions do not correspond to real fibre directions. Even if it is possible to describe the mechanical behaviour with this representation, the physical meaning is lost.

3.2. Green-Lagrange tensor components to describe anisotropy

An easy way to create an anisotropic constitutive equation is to write it as a sum of the contribution of the components of the strain tensor. Finally a weight is chosen for each component. As previously explained, soft tissues present an important strain hardening so an exponential form

Kaliske [71]	$W = \sum_k c_{k\geqslant 2}(I_4 - 1)^k$
Ruter et al. [78]	$W = \sum_{klmn} c_{klmn}(I_1 - 3)^k(I_2 - 3)^l(I_4 - 1)^m(I_5 - 1)^n$
Horgan et al [79]	$W = \sum_{klmn} c_{klmn}(I_1 - 3)^k \left[(I_2 - 3) - 3(I_1 - 3)\right]^l (I_4 - 1)^m(I_5 - 2I_4 + 1)^n$
Humphrey et al [80]	$W = \sum_{kl} c_{km}(I_1 - 3)^k \left(\sqrt{I_4} - 1\right)^m$
Jemolio et al [81]	$W = \sum_{klmn} c_{klmn}(I_1 - 3)^{a_k}(I_2 - 3)^{b_l}(I_4 - 1)^{c_m}(I_5 - 1)^{d_n}$
Jemolio et al [81]	$W = \sum_{klmn} c_{klmn}(I_1^{a_k} - 3^{a_k})(I_2^{b_l} - 3^{b_l})(I_4^{c_m} - 1)(I_5^{d_n} - 1)$

Table 1: Some infinite I_4, I_5 series developments proposed to model transverse isotropic soft tissues where a_k, b_k, c_k, d_k, c_{km} and c_{klmn} are material parameters (It is to note that c_{0010}=0, c_{0001}=0 for [78, 79]).

is often chosen. Fung and co-authors conducted several studies [59, 60, 61] using the following global form of SEDF $W = \frac{c}{2}(\exp Q - 1)$. Q is here a function of the strain components that can be written as $Q = A_{ijkl}E_{ij}E_{kl}$ where A_{ijkl} are material parameters. Different formulations were written in two and three dimensions. A review about the different equations can be found in [62]. These constitutive equations were often used for cardiovascular soft tissues (i.e. heart, arteries...) and are often written in cylindrical coordinates. Different constitutive equations have proved their efficiency for different biomedical applications. In this chapter, the example of Guccione et al [63] is selected. The constitutive equation for one fibre reinforcement is written as:

$$Q = b_f E_{11}^2 + b_t(E_{22}^2 + E_{33}^2 + E_{23}^2 + E_{32}^2) + b_{fs}(E_{12}^2 + E_{21}^2 + E_{13}^2 + E_{31}^2) \tag{8}$$

where b_f, b_t and b_{fs} are material parameters. It is to note that the exponential form is not the only that is used even if it is largely spread. Some other forms as polynomial [64, 65, 66] or inverse function [67] have also been proposed. For all these models, the main difficulty is that the material parameters have no physical meaning and their fit needs to be perform carefully [68, 69, 54].

3.3. Strain invariants formulation

3.3.1. Classical formulation

The idea is here to express the constitutive equation by means of all the invariants which are more numerous in an anisotropic context. A good way to describe any function is to use a series development. It represents a generalisation to anisotropy of Rivlin series [70]. Nevertheless, it is to note that different authors proposed to write the series developments in different ways. Some expressions are detailed in table 1. The term $k = 2$ of Kaliske model [71] corresponds to the standard reinforcing model [72, 73, 74, 75], not initially proposed for soft tissues but which represents the most simple function in I_4 that can be used. It is to note that the use of $\sqrt{I_4}$ permits to obtain a model that represents the behaviour of a linear spring with the quadratic formulation [76, 77]. As for isotropy, the series cannot be used in a infinite version and a main point to discuss is the choice of the terms that must be kept. Some discussions about particular cases are reported in [72, 82, 22, 80]. Let us mention that few SEDFs involving the I_5 invariant have been proposed. In most of the cases, expressions limited to I_4 are preferred. But the use of only I_4 or I_5, instead of the both invariants is a still questionable as it leads to the same shear modulus in direction and orthogonal to the reinforced direction [22]. Moreover today, no series development using I_8 was proposed.

The description of a behavior with strong strain hardening using polynomial SEDFs needs too many terms. To avoid this, other forms based on exponential functions were proposed. It consists in increasing largely the strain energy for the material when stretched in fibre direction. A first exponential constitutive equation was proposed by Humphrey and Yin [83]:

$$W = c_1(\exp(c_2(\sqrt{I_4} - 1)^2) - 1) \tag{9}$$

This expression was later expressed by means of I_4 instead of $\sqrt{I_4}$ by Holzapfel et al [54]:

$$W = \mu(I_1 - 3) + \frac{c_1}{2c_2}\left[\exp(c_2(I_4 - 1)^2) - 1\right] \tag{10}$$

This model was widely used for different soft tissues. Later, it has been extended to take into account the isotropic and anisotropic parts ratio by introducing a weighting factor between the contributions of I_1 and I_4 [84]. This factor κ represents a measure of dispersion in the fibre orientation (it is noted HGO model in the rest of the paper):

$$W = \mu(I_1 - 3) + \frac{c_1}{2c_2}\left\{\exp\left(c_2\left((1-\kappa)(I_1 - 3)^2 + \kappa(I_4 - 1)^2\right) - 1\right)\right\} \tag{11}$$

In the three previous SEDFs (9,10,11), μ, c_1, c_2 and κ are material parameters. The form of the term/s in the exponential function has/have largely evolved and many other expressions have been proposed. The reader can refer to [85, 86, 87, 88, 89, 90, 91] for example. Recently, a general form for the SEDF was proposed by Peña et al [92]:

$$W = \frac{\gamma}{a\eta}\left[\exp(\eta(I_1 - 3)^a) - f_1(I_1, a)\right] + \frac{c_i}{bd_i}[\exp(d_i(I_4^{(i)} - I_4^0)^b) - g(I_4^{(i)}, I_4^0, b)]. \tag{12}$$

The choice of the functions f_1 and g permits to generalise many different models. γ, η, a, b, c_i, d_i and I_4^0 are material parameters, I_4^0 represents the threshold to reach for the fibre to become loaded. To our knowledge, only few SEDF involving also I_5 was proposed for soft tissue [93]:

$$W = a(I_1 - 3) + b(I_2 - 3) + \frac{c_1}{2c_2}\left(\exp\left\{c_2(I_4 - 1)^2\right\} - 1\right) + \frac{c_3}{2c_4}\left(\exp\left\{c_4(I_5 - 1)^2\right\} - 1\right) \tag{13}$$

where a, b, c_1, c_2, c_3 and c_4 are material parameters. Even if this constitutive equation was initially developed for arteries [94, 95, 96], it was also used for different biological tissues, as for example human cornea [97], erythrocytes [98], the mitral valve [99], trachea [100, 101], cornea [102, 103], collagen [104], abdominal muscle [105].

Nevertheless, the constitutive equations for soft tissues could be written using other mathematical functions instead the exponential one. As for rubber like materials, several mathematical functions have been proposed. Using an exponential function supposes a strong strain hardening effect. To overcome such limitation several different constitutive equations can also be used for soft tissues as they present similar abilities. Some equations are detailed in table 2. It is to note that these equations developed for composite materials are also written with I_5. The first equations were proposed for soft tissues and use ln or tanh functions. The second part of the table lists a series of SEDFs that were proposed to describe the mechanical behaviour for fibres reinforced materials but not soft tissues. But as explained previously, many soft tissues are fibres reinforced materials as a consequence all these SEDFs could also be used for soft tissues and can bring new abilities for teh modelling.

Non classical constitutive equations with square root, tanh and ln functions.	
Dorfmann et al. [106]	$W = c_2 \left[1 - c_3 \tanh\left(\frac{I_4-1}{c_4}\right)\right]\left[\exp(c_5(I_4-1)^2) - 1\right]$
Limbert and Middleton [107]	$W = 2c_5\sqrt{I_4} + c_6 \ln(I_4)$
Calvo et al. [108]	$W = 2c_5\sqrt{I_4} + c_6 \ln(I_4) + c_7$
Constitutive equation initially developped for reinforced materials	
Horgan and Saccomandi [79]	$W_{,4} = -\frac{c_1+c_2(I_4-1)}{c_3+c_4(I_4-1)+c_5(I_4-1)^2+c_6(I_5-2I_4+1)}$
Horgan and Saccomandi [79]	$W_{,4} = -\frac{c_1+c_2(I_4-1)}{c_3+c_4(I_4-1)}$
Horgan and Saccomandi [79]	$W = -c_2c_3\left(I_4 - 1 + c_3 \ln\left(1 - \frac{I_4-1}{c_3}\right)\right)$
Horgan and Saccomandi [79]	$W = -\frac{c_2}{n}c_3 \ln\left(1 - \frac{(I_4-1)^n}{c_3}\right)$
Horgan and Saccomandi [79]	$W = -c_1c_2 \log\left(1 - \frac{(I_5-1)^2}{c_2}\right)$
Ruter and Stein [78]	$W = c_2\left(\cosh(I_4-1) - 1\right)$
Ogden and Saccomandi [109]	$W = -\frac{c_2}{2}c_3 \ln\left(1 - \frac{(I_4-1)^2}{c_3}\right)$
Markert et al. [110]	$W = \frac{c_1}{c_2}(I_4^{c_2/2} - 1) - c_1 \ln(I_4^{1/2})$
Demirkoparan et al [111, 112]	$W = \frac{2}{3}\left(\frac{I_4}{c_1^2} + 2\frac{c_1}{\sqrt{I_4}} - 3\right)$
Lurding et al. [113]	$W = c_1(I_1-3) + c_2(I_1-3)(I_4-1) + c_3(I_4^2 - I_5)$ $+c_4(\sqrt{I_4}-1)^2 + c_5 \ln(I_4)$
Chui et al. [113]	$W = c_1 \ln(1-T) + c_5(I_1-3)^2 + c_6(I_4-1)^2 + c_7(I_1-3)(I_4-1)$ with $T = c_2(I_1-3)^2 + c_3(I_4-1)^2 + c_4(I_1-3)(I_4-1)$

Table 2: Some original forms of constitutive equations using I_4 and I_5, where c_i with $i = 1...7$ are material parameters.

3.3.2. Coupling influence

The detailed SEDFs of the previous paragraphs do not take into account the coupling that can exist between the different fibre families. The additive decomposition that is used implies a superposition principle. A first way to create a coupling is to propose constitutive equations presenting multiplicative terms between the different directions. In this spirit, an anisotropic SEDF W with two fibre families was proposed for pneumatic membranes [114]:

$$W = c_1^{(1)}\left(I_4^{(1)}-1\right)^{\beta_1} + c_2^{(1)}\left(I_5^{(1)}-1\right)^{\beta_2} + c_1^{(2)}\left(I_4^{(2)}-1\right)^{\gamma_1} + c_2^{(2)}\left(I_5^{(2)}-1\right)^{\gamma_2}$$
$$+c_c^{(1)}\left(I_1-3\right)^{\delta_1}\left(I_4^{(1)}-1\right)^{\delta_1} + c_c^{(2)}\left(I_1-3\right)^{\delta_2}\left(I_4^{(2)}-1\right)^{\delta_2} + c_c^{(1,2)}\left(I_4^{(1)}-1\right)^{\eta}\left(I_4^{(2)}-1\right)^{\eta}. \quad (14)$$

This strain energy allows coupling between the different directions, but the additive decomposition of the constitutive equation permits to fit separately the different parameters $c_i^{(j)}$, δ_i and β_i. The coupling between the two directions is given by the parameter $c_c^{(1,2)}$. This series development can be imagined with any terms and any powers to change the coupling. More recently and in the same spirit, Holzapfel and Ogden [115] develop an interesting structurally based orthotropic model of the passive myocardium that accounts for muscle fibre direction and the myocyte sheet structure.

Another method consists in coupling invariants from different directions [37], a new quantity is created taking into account the contribution of the different directions, the following invariant expression was proposed:

$$\alpha^2 I_4^{(1)2} + 2\lambda(1-\alpha)I_4^{(1)}I_4^{(2)} + (1-\alpha)^2 I_4^{(2)2} \text{ with } \alpha \in [0,1]. \quad (15)$$

α represents a material parameter. This expression permits to measure the deformation in two directions with only one invariant. Nevertheless, this has not yet been used in constitutive equations. A simple additive decomposition of the invariants in a same function can create the coupling [116] and can be used [117] as in the exponential form:

$$W = \frac{c_1}{c_2}\left[\exp\left(c_2\left(I_4^{(1)}+I_4^{(2)}-2\right)\right) - c_2\left(I_4^{(1)}+I_4^{(2)}\right) + 2c_2 - 1\right]. \quad (16)$$

A generalised weighted expression of the constitutive equation was also developed [118, 119]:

$$W = \frac{1}{4}\sum_r \mu_r\left[\frac{1}{\alpha_r}\left(\exp\left(\alpha_r\left(\sum_i \gamma_i I_4^{(i)}-1\right)\right)-1\right) + \frac{1}{\beta_r}\left(\exp\left(\beta_r\left(\sum_i \gamma_i P_5^{(i)}-1\right)\right)-1\right)\right]. \quad (17)$$

with $P_5 = \mathrm{tr}(\mathrm{Cof}(\mathbf{C})\mathbf{A}^{(i)})$ where Cof is the cofactor operator, μ_r, β_r, γ_i and α_r are material parameters.

These models are coupling the stretches of the different fibres but do not take into account the shear in the matrix due to the presence of fibres. To handle such limitation we need to account for $I_8^{(i,j)}$ and $I_9^{(i,j)}$. The idea is thus to add terms in the strain energy taking into account these invariants. Few constitutive equations were proposed in the literature, but one example was proposed for oesophageal tissues where a quadratic function was added [120]:

$$\begin{aligned} W &= \tfrac{c_1}{c_3}\exp[c_3(I_1-3)] + \tfrac{c_2}{c_5}\exp[c_5(I_2-3)] \\ &+ \tfrac{c_4}{c_7^2}\left\{\exp[c_7(I_4^{(1)}-1)] - c_7(I_4^{(1)}-1) - 1\right\} \\ &+ \tfrac{c_6}{c_8^2}\left\{\exp[c_8(I_4^{(2)}-1)] - c_8(I_4^{(2)}-1) - 1\right\} + c_9\left[I_8^{(1,2)} - I_9^{(1,2)}\right]^2, \end{aligned} \quad (18)$$

where c_i with $i = 1...9$ are material parameters. For annulus fibrous tissues, the influence of the interaction between the layers was modelled [121] with a term taking into account $I_4^{(1)}$, $I_4^{(2)}$ and $I_8^{(1,2)}$:

$$W = \frac{c_1}{2c_2}\left(\exp\left(c_2\left(\frac{I_8^{(1,2)}}{\left(I_4^{(1)}I_4^{(2)}I_9^{(1,2)}\right)^{1/2}} - \sqrt{I_9^{(1,2)}}\right)^2\right) - 1\right). \tag{19}$$

A similar form from exponential model was proposed also for I_8 [122]:

$$W = \frac{c_1}{c_2}\left[\exp\left(c_2\frac{\left(I_8^{(1,2)}\right)^2}{I_9^{(1,2)}}\right) - 1\right]. \tag{20}$$

In the two previous models c_1 and c_2 are material parameters. Few invariant-coupling models were used for biological tissues, but they are proposed for composite material [123, 124]. In comparison with other models, these approaches take into account the shear strain in the material whereas the first models couple the deformations of the different fibres.

In a classical approach, as in plasticity or viscoelasticity, one proposes to decompose the strain energy into three parts $W = W^m + W^f + W^{fm}$ [125], where the three terms are the strain energy of the matrix, of the fibres and of the interactions between fibres and matrix, respectively. The decomposition of the strain energy function into different parts permits to analyse the loading states and to propose constitutive equations reproducing the strain endured by the fibre, the matrix and the interface. This leads to the construction of different function families [126]:

$$\begin{cases} W^m = \frac{1}{2}c_1 f(I_4)(I_1 - 3), \\ W^f = c_1 g_1(I_4)\left(\frac{I_5 - I_4^2}{I_4}\right), \\ W^{fm} = c_1 g_2(I_4)\left(I_1 - \frac{I_5 + 2\sqrt{I_4}}{I_4}\right). \end{cases} \tag{21}$$

Another basic form was also proposed for the interaction between the fibres and the matrix [125]:

$$W^{fm} = g_2(I_4)\left[\frac{I_4}{I_3}(I_5 - I_1 I_4 + I_2) - 1\right]^2, \tag{22}$$

where f, g_1 and g_2 are functions to define and c_1 is a material parameter. The first function corresponds a generalisation of the neo-Hookean model [127]. Few functions for f, g_1 and g_2 have been proposed for the moment, the first propositions are based on exponential functions [126, 128, 129].

4. About some specific constitutive equations

In this section, two well known constitutive equations, one expressed in term of strain components [63] and the other in term of strain invariants [84] are detailed on classical uniaxial mechanical tests.

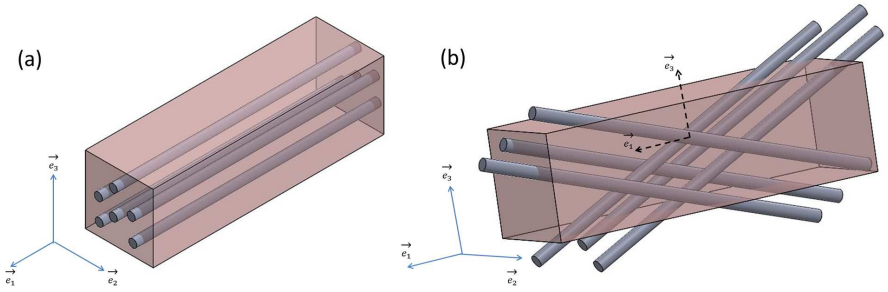

Figure 1: Representation of the orientation of the fibres for the two examples (a) uniaxial fibre reinforcement for Guccione et al model (b) biaxial fibre reinforcement for HGO model.

4.1. Transversely isotropic model of Guccione et al.

For this first example, a soft tissue with one reinforcement fibre orientation is considered as presented in figure 1(a). The fibres are oriented along direction 1. The equation of the model is presented in eq (8). Three uniaxial tensile tests are simulated in each direction of the framework (i.e. 1, 2 and 3). The stress-strain relationships are directly obtained by derivation of the energy density by each Green-Lagrange component. The uniaxial tension in direction 1 is easy to obtain as the behaviour of directions 2 and 3 are identical, the strain in these two directions is imposed by the incompressibility and the Lagrange multiplier unknown (which ensures incompressibility) is obtained to impose zero stress in these directions. For tension tests in direction 2 (or 3), the problem is slightly more complicated, as the strain in the two other directions are not identical due to the presence of fibres. A minimizing problem is written to ensure incompressibility and to impose zero stress in the two other directions.

The parameters used for the simulations are those proposed in [63], i.e. $c = 0.876$kPa, $b_f = 18.48$, $b_t = 3.58$ and $b_{fs} = 1.627$. The three curves corresponding to an uniaxial tensile test in each direction are presented in figure 2 (a). The curves present the Cauchy stress in function of the logarithmic strain. To highlight the strain hardening of the material, the slopes of the curve, i.e. the tangent moduli are also plotted in figure 2 (b). The tangent modulus is calculated by the slope of the Cauchy stress, logarithmic strain curve. It strongly appears that the moduli and especially the one in fibre direction are rapidly evolving with the strain. A linearization of the stress-strain relationships allows us to obtain the analytical expressions of whole initial material constants:

$$E_1 = \frac{c}{2}\left(2b_f + b_t\right), \tag{23}$$

$$E_2 = E_3 = \frac{cb_t\left(2b_f + b_t\right)}{\left(b_f + b_t\right)}. \tag{24}$$

By calculating the ratio between the different strains, the initial Poisson ratios can be obtained:

$$\nu_{12} = \nu_{13} = 0.5, \tag{25}$$

$$\nu_{31} = \nu_{21} = \frac{b_t}{\left(b_f + b_t\right)}, \tag{26}$$

$$\nu_{12} = \nu_{13} = \frac{b_f}{\left(b_f + b_t\right)}. \tag{27}$$

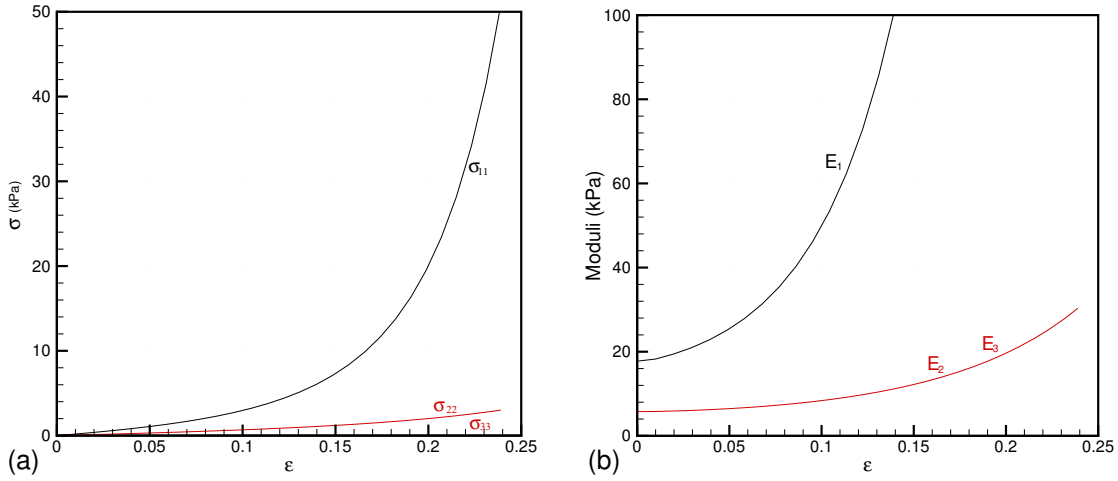

Figure 2: Guccione et al model (a) representation of the strain-stress curves for three different tensile tests, (b) representation of the tangent moduli for the same tests (ε is the Green-Lagrange strain and σ the Cauchy stress).

By simulating shear tests, the initial shear moduli can also be obtained:

$$\mu_{12} = \mu_{13} = \frac{cb_f}{2} \tag{28}$$

$$\mu_{23} = \frac{cb_t}{2} \tag{29}$$

It is important to notice that these initial material parameters are no longer constant values in large strains and thsee relationships (cf. Eq 23-29) are only valid for strain amplitudes lower than approximately 2%. However, one can take advantage of such relationships, to improve the performance of the identification method that needs to be conducted to obtain the material parameters from experimental data. Two steps are necessary to obtain the material constants. In a first step, one can use these linear relationships to quantify some material constants based on the small strain experimental responses. In the second step, the previous determined set of initial material constants can be used to partially initiate the optimization process conducted on the entire experimental responses including in the large strain domains.

4.2. HGO orthotropic model

In this section, a material presenting two reinforced directions is used. A representation of the material is presented in figure 1(b). The two fibre families are in the plane (1-3), they are symmetric with respect to the plane (2-3) and present an angle ϕ relative to axe 1. The equation of the HGO model was presented previously (eq 11). The parameters identified for media artery are used, $\mu = 1.27$kPa, $k_1 = 21.6$kPa, $k_2 = 8.21$, $\phi = 20.61$, $\rho = 0.25$ [84]. Different hypotheses exist in the literature about the contribution of the fibres in compression; some consider that they act whereas some consider that they do not contribute to the stress. In this example, it is considered that the fibres can be compressed and have the same parameters as in tension. The

same simulations as in the previous section are performed, i.e. three uniaxial tensile tests in the three axis 1, 2 and 3. Due to the orientation of the fibres, a minimizing scheme is necessary for each test (the transverse strains should verify the incompressibility hypothesis and the stress null in the transverse directions). A simulation of the three tensile tests is presented in figure 3 (a). Moreover, the tangent moduli are also presented in figure 3 (b). The conclusions are similar to the

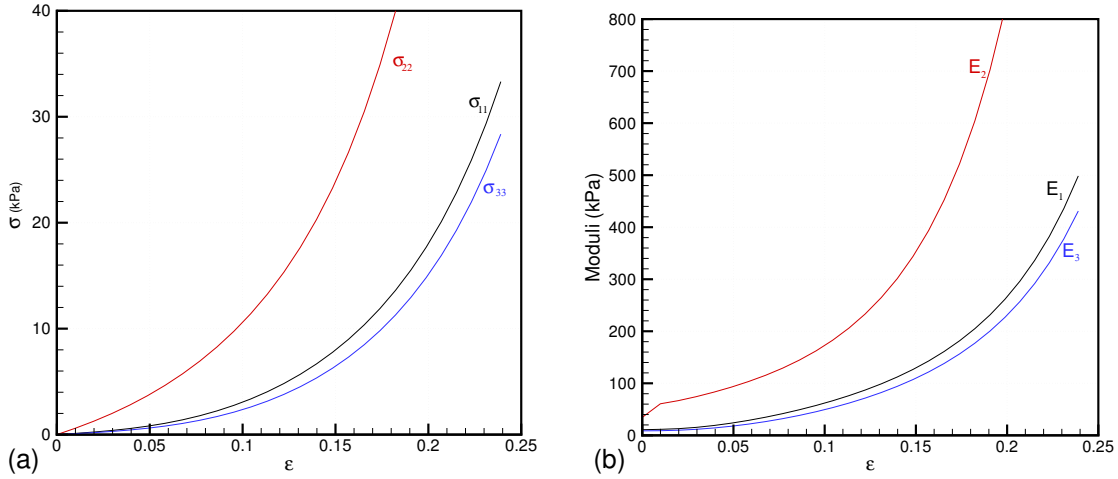

Figure 3: HGO model (a) representation of the strain-stress curves for three different tensile tests, (b) representation of the tangent moduli for the same tests (ε is the Green-Lagrange strain and σ the Cauchy stress).

previous model with tangent moduli that are increasing exponentially with strain. As previously, the linearization permits to determine the initial moduli and Poisson ratio, and the following values can be obtained:

$$E_1 = 2\mu \frac{3\mu + 4k_1\rho\left(\sin^4\phi + \cos^4\phi - \sin^2\phi\cos^2\phi\right)}{\mu + k_1\rho\left(\sin^2\phi - \cos^2\phi\right)^2}, \tag{30}$$

$$E_2 = 2\mu \frac{3\mu + 4k_1\rho\left(\sin^4\phi + \cos^4\phi - \sin^2\phi\cos^2\phi\right)}{\mu + k_1\rho\sin^4\phi}, \tag{31}$$

$$E_3 = 2\mu \frac{3\mu + 4k_1\rho\left(\sin^4\phi + \cos^4\phi - \sin^2\phi\cos^2\phi\right)}{\mu + k_1\rho\cos^4\phi}, \tag{32}$$

$$\nu_{12} = \frac{\mu - 2k_1\rho\sin^2\phi\left(\cos^2\phi - \sin^2\phi\right)}{2\left(\mu + k_1\rho\left(\sin^2\phi - \cos^2\phi\right)^2\right)}, \tag{33}$$

$$\nu_{23} = \frac{\mu + 2k_1\rho\sin^2\phi\cos^2\phi}{2\left(\mu + k_1\rho\sin^4\phi\right)}, \tag{34}$$

$$\nu_{32} = \frac{\mu + 2k_1\rho\sin^2\phi\cos^2\phi}{2\left(\mu + k_1\rho\cos^4\phi\right)}. \tag{35}$$

In the same way as tangent moduli, the Poisson ratios are evolving with the strain and are affected by the energy to compress the fibres. As previously pointed out at the end of the section 4.1, the performance of the identification method that needs to be conducted to obtain the material parameters from experimental data could be improved by taking advantage of such relationships.

4.3. About the two models

These two constitutive equations, even if they are not written in the same formalism, present very similar tendencies. It is to note that these models are elaborated to present an important strain hardening leading to a large increase of the tangent moduli when the material is stretched. Even if links with the initial moduli exists, these links should be used very carefully. They cannot be used to fit the model, these values are not constant for the models. They represent a linearization at the starting point. Moreover, it is often very difficult to obtain the experimental data near zero deformation due to experimental errors and due to the difficulty to identify the zero configuration of the samples. Nevertheless, the values of these linearized parameters highlight that the parameters of the models act on every components of the elasticity tensor and thus on the tangent elastic tensor.

A key point in the modelling is to define when the fibres start to resist when stretched. Many authors considered that the fibres must reach a threshold before opposing a stress. In this way, a threshold parameter can be introduced in all the constitutive equations presented in this review. It consist in replacing (I_4-1) by $(I_4-I_4^0)$, or $(\sqrt{I_4}-1)$ by $(\sqrt{I_4}-\sqrt{I_4^0})$ into the constitutive equations. I_4^0 corresponds to the needed deformation to generate stress, see for example [84, 92, 108, 130]. This new parameter permits to control easily the beginning of the strain hardening. Its value strongly depends on the choice of the reference on the zero state of the experimental data. This zero state is always difficult to identify and vary between post-mortem and in-vivo states and can depend on the person who performs the test. The addition of such parameter can strongly influence the figures presented in this paragraph.

According to the hypothesis that is used with the fibres in compression (they generate or not stresses), some strong changes of slopes can also be observed when the fibres change of loading (tension to compression or compression to tension). This phenomenon can appear even in monotonic loadings due to the rotation of the fibres during the deformation process.

5. How to account for a kinematics constraint in a constitutive law?

In this example, we illustrate how a kinematics constraint may be explicitly included in a passive stress-strain constitutive law. Extrapolations from cardiac muscle fibre arrangement to myocardial stress are realistic when we also account for the effects of the connective tissue. It is hypothesized that a part of that connective tissue, surrounding group of myocytes, affects the stress in the perpendicular direction of the muscle fibres running on the tangential plane of the ventricular wall. Based on the previous scanning electron microscope observations [131], we proposed a connective tissue organization illustrated in Fig. 4. We assumed that the myocytes are roughly cylindrical and that two oriented groups of myocytes (idealized as two cardiac fibres) are surrounded by inextensible collagen networks. So, during the passive compression in the fibre direction of an incompressible myocardial sample, the myocyte diameters increase and because the surrounding "belts" of collagen are inextensible, the adjacent muscle cells become closer. Such kinematic relation between the muscle fibre and cross-fibre extension ratios (named λ_{f_0} and $\lambda_{f_0^\perp}$, respectively) is given by:

$$h\left(\lambda_{f_0},\lambda_{f_0^\perp}\right)=1-\lambda_{f_0^\perp}+\frac{a}{D}(\pi-2)\left(1-\lambda_{f_0^\perp}^{-1/2}\right)=0 \tag{36}$$

with $D=4a+d$ where a is the initial myocyte radius and d is the initial distance between the two cells (Fig. 4). Notice that this kinematics constraint exists only if the cardiac fibre is under

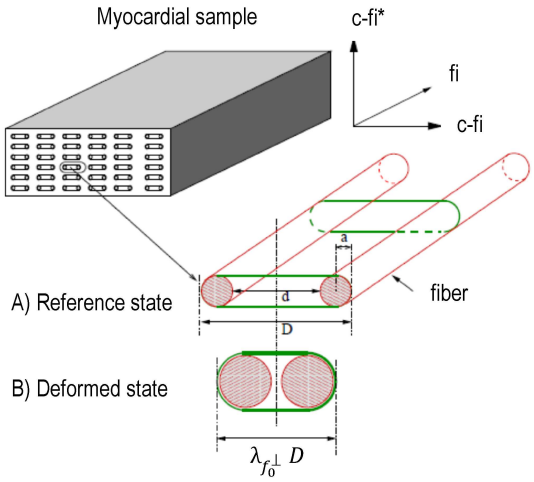

Figure 4: Schematic illustrations of a myocardial sample and the kinematic constraint induced by the collagen network surrounding the muscle fibres. A) Before compression (reference state). B) After or during the uniaxial compression in the fibre direction (deformed state). **fi**: fibre direction define by the unit vector $\mathbf{f}_0$; $\mathbf{c}-\mathbf{fi}$: cross-fibre direction in the tangential plane define by the unit vector $\mathbf{f}_0^\perp$); $\mathbf{c}-\mathbf{fi}^*$: cross-fibre direction perpendicular to the tangential plane (adapted from [133]).

compression (i.e. if $\lambda_{f_0} < 1$). In terms of strain invariants, this kinematics constraint becomes:

$$h\left(I_{4f_0}, I_{4f_0^\perp}\right) = 1 - I_{4f_0^\perp}^{1/2} + \frac{a}{D}(\pi - 2)\left(1 - I_{4f_0^\perp}^{-1/4}\right) = 0 \quad \text{if} \quad I_{4f_0} < 1 \tag{37}$$

with

$$I_{4f_0} = \mathbf{f_0} \cdot (\mathbf{C}\mathbf{f_0}) \quad \text{and} \quad I_{4f_0^\perp} = \mathbf{f_0^\perp} \cdot \left(\mathbf{C}\mathbf{f_0^\perp}\right) \tag{38}$$

where $\mathbf{f_0}$ and $\mathbf{f_0^\perp}$ are two unit vectors given in the reference configuration. These vectors are parallel and perpendicular to the muscle fibres, respectively. Both vectors are running on the tangential plane of the ventricular wall. To satisfy this kinematic constraint the SEDF of the passive incompressible tissue needs to be split into a material term $W_{mat}(\mathbf{E})$ and a kinematics contribution $W_{kin}(\mathbf{E})$:

$$W(\mathbf{E}) = W_{mat}(\mathbf{E}) + W_{kin}(\mathbf{E}) \tag{39}$$

with :

$$W_{kin}(\mathbf{E}) = -\frac{1}{2} q h\left(I_{4f_0}, I_{4f_0^\perp}\right) \tag{40}$$

The scalar function q introduced in Eq. 40 serves as an additional indeterminate Lagrange multiplier to insure the kinematics condition given by Eq. 37. As a result, the expression of the Cauchy stress tensor σ, is given by (see Chapter 2 of this book):

$$\sigma = \mathbf{F}\frac{\partial W_{mat}(\mathbf{E})}{\partial \mathbf{E}}\mathbf{F}^T + \sigma_{kin} - p\mathbf{I} \tag{41}$$

with

$$\sigma_{kin} = \mathbf{F}\frac{\partial W_{kin}\left(\mathbf{E}\right)}{\partial \mathbf{E}}\mathbf{F}^T = -q\left[\frac{\partial h\left(I_{4f_0}, I_{4f_0^\perp}\right)}{\partial I_{4f_0}}\mathbf{f}\otimes\mathbf{f} + \frac{\partial h\left(I_{4f_0}, I_{4f_0^\perp}\right)}{\partial I_{4f_0}^\perp}\mathbf{f}^\perp\otimes\mathbf{f}^\perp\right] \tag{42}$$

and

$$\frac{\partial h\left(I_{4f_0}, I_{4f_0^\perp}\right)}{\partial I_{4f_0}} = \frac{a}{4D}(\pi-2)I_{4f_0}^{-5/4} \tag{43}$$

$$\frac{\partial h\left(I_{4f_0}, I_{4f_0^\perp}\right)}{\partial I_{4f_0}^\perp} = -\frac{1}{2}I_{4f_0^\perp}^{-1/2} \tag{44}$$

where $\mathbf{f} = \mathbf{F}\mathbf{f}_0$, $\mathbf{f}^\perp = \mathbf{F}\mathbf{f}_0^\perp$, p is a second Lagrange multiplier associated with the kinematics incompressibility constraint $\det(\mathbf{F}) = 1$, and $\mathbf{I}$ is the identity matrix. An extended active version of this model has been proposed to explain the observed left ventricular wall thickening during the ejection phase of the cardiac cycle [132, 133].

6. Passive hyperelastic SEDFs used in the book chapters

In this book, several strain energy density functions (*SEDFs*) were used to model biological tissues. For compressible and quasi-incompressible media the *SEDF* can be given in decoupled form as:

$$W\left(\boldsymbol{C}\right) = W_{iso}\left(\bar{\boldsymbol{C}}\right) + W_{vol}\left(J\right)$$

where W_{vol} and W_{iso} are *SEDFs* describing the volumetric and isochoric response of the material, respectively, J is the volume ratio ($J = \det \boldsymbol{F}$, where $\boldsymbol{F}$ is the deformation gradient), $\boldsymbol{C} = \boldsymbol{F}^T \cdot \boldsymbol{F}$ is the right Cauchy-Green strain tensor and $\bar{\boldsymbol{C}} = J^{-2/3}\boldsymbol{C}$ is the modified right Cauchy-Green strain tensor. Once we know the form of the *SEDF*, the 2nd Piola-Kirchhoff stress tensor can be derived [134] as:

$$\boldsymbol{S} = \boldsymbol{S}_{iso} + \boldsymbol{S}_{vol},$$

with $\boldsymbol{S}_{vol} = 2\frac{\partial W_{vol}}{\partial J}\frac{\partial J}{\partial \boldsymbol{C}}$ and $\boldsymbol{S}_{iso} = 2\frac{\partial W_{iso}}{\partial \bar{\boldsymbol{C}}} : \frac{\partial \bar{\boldsymbol{C}}}{\partial \boldsymbol{C}}$. For purely incompressible material ($J = 1$), the 2nd Piola-Kirchhoff stress tensor adopts the following form:

$$\boldsymbol{S} = 2\frac{\partial W_{iso}}{\partial \boldsymbol{C}} - p\boldsymbol{C}^{-1}$$

where p is the Lagrange multiplier introduced to enforce incompressibility. In the Table 3 one lists the main passive hyperelastic *SEDFs* $W_{iso}(\boldsymbol{C})$, used in this book to model the biomechanical behavior of living organs, when assuming purely incompressible biological tissues. The SEDFs for quasi-incompressible biological tissues are, in general, given as function of the invariants referred to $\boldsymbol{C}$ (here denoted $I_k, k = 1, ..., 5$ and $k = 8$). However, in literature some SEDFs are given with the help of the invariants referred to $\boldsymbol{E}$ (here denoted $I_k^*, k = 1, ..., 5$ and $k = 8$). The relationship between these two families of invariants is:

$$
\begin{aligned}
I_1^* &= Tr\left(\boldsymbol{E}\right) = \frac{1}{2}\left(I_1 - 3\right) \\
I_2^* &= \frac{1}{2}\left(Tr\left(\boldsymbol{E}\right)^2 - Tr\left(\boldsymbol{E}^2\right)\right) = \frac{1}{4}\left(-2I_1 + I_2 + 3\right) \\
I_3^* &= \det \boldsymbol{E} = \frac{1}{8}\left(I_1 - I_2 + I_3 - 1\right) \\
I_4^* &= \boldsymbol{E}\colon \boldsymbol{f} \otimes \boldsymbol{f} = \frac{1}{2}\left(I_4 - 1\right) \quad \text{with } \boldsymbol{f} \cdot \boldsymbol{f} = 1 \\
I_5^* &= \boldsymbol{E}^2\colon \boldsymbol{f} \otimes \boldsymbol{f} = \frac{1}{4}\left(I_5 - 2I_4 + 1\right) \\
I_8^* &= \boldsymbol{E}\colon \boldsymbol{f} \otimes \boldsymbol{s} = \frac{1}{2}I_8, \quad \text{with } \boldsymbol{f} \cdot \boldsymbol{s} = 0
\end{aligned}
$$

Organs/Chapters	**Orthotropic SEDFs**
Coronary /2, 9 Aorta/8	Holzapfel et al., 2005,*Am J Physiol*, 289:H2048-2058 $W = \mu\,(I_1 - 3) + \sum_{i=1}^{2} \frac{k_1}{2k_2} \left\{ \exp\left[k_2 \left((1-\rho)\,(I_1 - 3)^2 + \rho\,(I_{4i} - 1)^2 \right) \right] - 1 \right\}$
Skin/16	Holzapfel et al., 2001, *J. Elasticity* 61:1-48 $W = \frac{\mu}{2}(I_1 - 3) + \mu \sum_{i=1}^{2} \frac{k_{i1}}{2k_{i2}} \left\{ \exp\left[k_{i2}(tr(\boldsymbol{H}_i \cdot \boldsymbol{C}) - 1)^2 \right] - 1 \right\}$ with $\boldsymbol{H}_i = \kappa_i \boldsymbol{I} + (1 - 3\kappa_i)\boldsymbol{e}_1 \otimes \boldsymbol{e}_2$
Esophagus/7 Aorta/8 Small intestine/13	Fung et al.,1979. *Am J of Physiology*, 237:H620-H631 $W = \frac{C}{2} \left\{ \exp\left(Q \right) - 1 \right\}$ with $Q = a_1 E_{\theta\theta}^2 + a_2 E_{zz}^2 + a_3 E_{rr}^2 + 2a_4 E_{\theta\theta} E_{zz}$ $+2a_5 E_{zz} E_{rr} + 2a_6 E_{\theta\theta} E_{rr} + a_7 E_{\theta z} E_{z\theta} + a_8 E_{rz} E_{zr} + a_9 E_{r\theta} E_{\theta r}$
Heart/2	Holzapfel and Ogden, 2009. *Philos Trans A Math Phys Eng Sci.* 367:3445-3475 $W = \frac{a_0}{2b_0} \left\{ \exp\left[b_0\,(I_1 - 3) \right] - 1 \right\} + \frac{a_f}{2b_f} \left\{ \exp\left[b_f\,(I_{4f} - 1)^2 \right] - 1 \right\}$ $+ \frac{a_s}{2b_s} \left\{ \exp\left[b_s\,(I_{4s} - 1)^2 \right] - 1 \right\} + \frac{a_{fs}}{2b_{fs}} \left\{ \exp\left[b_{fs} I_{8fs}^2 \right] - 1 \right\}$
Esophagus/7	Sommer et al., 2013. *Acta Biomater.* 9:9379-9391 $W = \mu(I_1 - 3) + W_{ani}$ with $W_{ani} = \frac{k_1}{2k_2} \sum_{i=1}^{2} \left\{ \exp\left[k_2 (I_{4i} - 1)^2 \right] - 1 \right\}$
Aorta/8	Gasser et al., 2006, *JR Soc Interface*, 3:15-23 $W = c_0(I_1 - 3) + \sum_{i=1}^{N} c_1 \left\{ \exp\left[c_2 E_i^2 \right] - 1 \right\}$ with $E_i = (\kappa \boldsymbol{I} + (1 - 3\kappa)\boldsymbol{f}_i \otimes \boldsymbol{f}_i) : \boldsymbol{C} - 1$
Aorta/8	Holzapfel and Gasser, 2001. *Comp. Meth. Appl. Mech. Eng.* 190:4379-4403 $W = c_0(I_1 - 3) + \sum_{i}^{N} c_{1i} \left\{ \exp\left[c_{2i} (I_{4i} - 1)^2 \right] - 1 \right\}$
Aorta/8	Basciano and Kleinstreuer, 2009. *J. Biomech.* Eng. 131:021009 $W = c_0(I_1 - 3) + \sum_{i=1}^{2} c_1 (I_{4i} - 1)^6$
Aorta/8	Celi and Berti, 2012, in Biomechanics and modeling of aneurysm, Murai Y. Ed. in Tech $W = \sum_{i=1}^{3} c_{0i} (I_1 - 3)^i + \sum_{i=1}^{2} c_{1i} (I_{4i} - 1)^i$

Organs/Chapters	**Transversely isotropic SEDFs**
Heart/2, 21	$W = \frac{C}{2}\left[\exp Q - 1\right]$, (Fung et al.,1979. *Am J of Physiology*, 237:H620-H631) Guccione et al., 1991. *J. Biomech. Engineering* , 113:42-55 $\begin{aligned} Q &= c_2 E_{ff}^2 + c_3\left(E_{ss}^2 + E_{nn}^2 + 2E_{sn}E_{ns}\right) + 2c_4\left(E_{fs}E_{sf} + E_{fn}E_{nf}\right) \\ &= c_3\left(I_1^{*2} + 2I_2^*\right) + (c_2 - c_3)I_4^* + 2(c_4 - c_3)I_5^* \end{aligned}$
Heart/21	Bovendeerd et al. 1992, *J. Biomech* 25:1129-1140 $\begin{aligned} Q &= a_1\left(E_{ss}^2 + E_{nn}^2\right) + (a_1 + a_2)E_{ff}^2 + 2a_1\left(E_{fs}E_{sf} + E_{sn}E_{ns} + E_{fn}E_{nf}\right) \\ &= a_1\left(I_1^{*2} + 2I_2^*\right) + a_2 I_4^* \end{aligned}$
Abdomen/12	Calvo et al., 2009. *J. Biomech* 42:642-651 $W = c_1(I_1 - 3) + W_{ani}$ $W_{ani} = \begin{cases} 0 & I_4 < I_{40} \\ \frac{c_3}{c_3}\left\{\exp\left[c_4(I_4 - I_{40})\right] - c_4(I_4 - I_{40}) - 1\right\} & I_{40} < I_4 < I_{4ref} \\ c_5\sqrt{I_4} + \frac{c_6}{2}\ln I_4 + c_7 & I_4 > I_{4ref} \end{cases}$
Aorta/8	Riveros et al., 2013, *Ann. Biomed. Eng.* 41:694-708 $W = c_0\left\{\exp\left[c_1(I_1 - 3)\right] - 1\right\} + c_2\left\{\exp\left[c_3(I_4 - 1)\right] - 1\right\}$
Heart/21	Based on Kerckhofs et al., 2003. *Ann Biomed Eng* 31:536-547 and Bovendeerd et al., 2009. *Am J Physiol* 297:H1058-H1068 $\begin{aligned} W &= a_0\left(\exp Q - 1\right) + a_3\left(\exp\left\{a_4 E_{ff}^2\right\} - 1\right) \quad \text{with } E_{ff}^2 = I_5^* \\ Q &= a_1\left(E_{ff}^2 + E_{ss}^2 + E_{nn}^2\right) + 2a_1 E_{sn}E_{ns} + (2a_1 + a_2)\left(E_{fs}E_{sf} + E_{fn}E_{nf}\right) \\ &= a_1\left(I_1^{*2} + 2I_2^*\right) + a_2 I_5^* \end{aligned}$
Breast/10	Han et al., 2014. *IEEE Transactions on Medical Imaging* 33(3): 682-694 $W = \frac{\mu}{2}\left(I_1 - 3\right) + \frac{\eta}{2}\left(I_4 - 1\right)^2$
Skeletal muscle/17	Blemker et al. this book $W = G_1\left(\frac{I_5}{I_4} - 1\right) + G_2\left(\cosh^{-1}\left\{\frac{I_1 I_4 - I_5}{2\sqrt{I_4}}\right\}\right)^2$

Organs/Chapters	**Isotropic SEDFs**
	General form of the polynomial model (including Neo-Hookean Yeoh and Mooney-Rivlin models) $W = \sum_{i+j>0} C_{ij} \left(I_1 - 3\right)^i \left(I_2 - 3\right)^j$
Skin/16	Hendriks et al., 2003. *Skin Research and Technology*, 9:274-283 $W = C_{10} \left(I_1 - 3\right) + C_{01} \left(I_2 - 3\right) + C_{11} \left(I_1 - 3\right) \left(I_2 - 3\right) + C_{20} \left(I_1 - 3\right)^2 + C_{30} \left(I_1 - 3\right)^3$
Tongue/19	Gerard et al., 2003. *Recent Research Developments in Biomechanics, Transworld Research Network*, 1:49-64 $W = C_{10} \left(I_1 - 3\right) + C_{01} \left(I_2 - 3\right) + C_{11} \left(I_1 - 3\right) \left(I_2 - 3\right) + C_{20} \left(I_1 - 3\right)^2 + C_{02} \left(I_2 - 3\right)^2$
Brain/6	Laskari et al., 2012. *J. Biomech.*, 45:642-646 $W = C_{10} \left(I_1 - 3\right) + C_{01} \left(I_2 - 3\right) + C_{11} \left(I_1 - 3\right) \left(I_2 - 3\right)$
Brain/6 Tongue/19	Schiavone et al., 2009. *Medical Image Analysis*, 13:673-678 $W = C_{10} \left(I_1 - 3\right) + C_{30} \left(I_1 - 3\right)^3$
Calf/24 (deep tissue) Tongue/20,19 Face/20,18	$W = C_{10} \left(I_1 - 3\right) + C_{20} \left(I_1 - 3\right)^2$
Larynx/20	$W = C_{01} \left(I_2 - 3\right) + C_{20} \left(I_1 - 3\right)^2$
Liver/11	N=2, Fu et al., 2013, *J. Mech Behav Biomed Mater.* 20:105-112 N=3, Umale et al., 2013. *J. Mech Behav Biomed Mater.* 17:22-33
Tongue/19	Wilhelms-Tricarico, 1995. *J. Acoust. Soc. Am*, 97:3085-3098 $W = c_0 \left\{ \exp \left[c_1 \left(I_1 - 3\right)^2 + c_2 \left(-2I_1 + I_2 + 3\right) \right] - 1 \right\}$

Organs/Chapters	**Isotropic SEDFs**, continued
Breast/10 - Uterus/15 - Foot/25 (heel,skin, fat, muscle) - Calf/24 (surface tissue) Spine/22 (Ground substance of annulus bulk, nucleus pulposus)	Neo-Hookean: $W = C_{10}\left(I_1 - 3\right)$
Thigh/23 Face/18 - Tongue/19 Spine/22 (Ground substance of annulus bulk, nucleus pulposus)	Mooney-Rivlin $W = C_{10}\left(I_1 - 3\right) + C_{01}\left(I_2 - 3\right)$
Liver/11 Spine/22 (ground substance of annulus bulk) Aorta/8	Yeoh model $W = \sum_{k=1}^{N} C_k \left(I_1 - 3\right)^k$
Skin/16 - Liver/11 - Rectum/14 - Bladder/14 - Spine/22 (Ligaments)	Ogden model $W = \sum_{k}^{N} \frac{\mu_k}{\alpha_k}\left(\lambda_1^{\alpha_k} + \lambda_2^{\alpha_k} + \lambda_3^{\alpha_k} - 3\right)$
Aorta/8	Ogden, 1972. *Proc. R. Soc. Lond. A* 326:565-584 $W = c_0 \sum_{k=1}^{3}(\lambda_k^4 - 1)$
Liver/11	Bogen model (special case of the Ogden model) $W = \frac{\mu}{\alpha}\left(\lambda_1^{\alpha} + \lambda_2^{\alpha} + \lambda_3^{\alpha} - 3\right)$
Liver/11 Aorta/8 Tongue/19	Demiray, 1981. *J. Biomech. Eng.* 103:73-78 $W = \frac{C_1}{2C_2}\left\{\exp\left[C_2\left(I_1 - 3\right)\right] - 1\right\}$

Organs/Chapters	**Isotropic SEDFs**, continued
Tongue/25	Whilems-Tricarico, 1995. *J. Acout. Soc. Am.* 97:3085-3098 $W = c_0 \left(\exp\left[c_1(I_1-3)^2 + c_2(-2I_1+I_2+3)\right]-1\right)$
Liver/11	Logarithmic model $W = -C_1 \ln\left\{1 - C_2\left(\lambda_1^{\alpha_1} + \lambda_2^{\alpha_2} + \lambda_3^{\alpha_3} - 3\right)\right\}$
Liver/11	Exponential model $W = C_1\left\{\exp\left[C_1\left(\lambda_1^{\alpha_1} + \lambda_2^{\alpha_1} + \lambda_3^{\alpha_1} - 3\right)\right] - 1\right\}$
Liver/11	Veronda and Westmann, 1970. *J. Biomech.* 3:111-124 $W = C_1\left\{\exp\left[C_3(I_1-3)\right]-1\right\} + C_2\left(I_2-3\right)$
Skin/16	Gambarotta et al., 2005. *J. Biomech.* 38:2237-2247 $W = a_1 I_1^{*2} + a_2 I_2^* + a_3 \exp\left[a_4 I_1^{*2} + a_5 I_2^*\right]$

Table 3: **Non exhaustive list of passive hyperelastic *SEDFs* presented in this book to model the biomechanics of living organs**. $I_i\left(\boldsymbol{C}\right), i = 1,2,3$ are the invariants of the right Cauchy-Green tensor; $I_{4i} = \boldsymbol{C}\colon\left(\boldsymbol{f}_i \otimes \boldsymbol{f}_i\right)$ is the 4^{th} invariant given by the contraction of $\boldsymbol{C}$ and the structural tensor $\boldsymbol{f}_i \otimes \boldsymbol{f}_i$ where $\boldsymbol{f}_i$ is the direction of the i^{th} family of fibers in the reference configuration; similarly, we define the 5^{th} invariant as $I_{5i} = \boldsymbol{C}^2\colon\left(\boldsymbol{f}_i \otimes \boldsymbol{f}_i\right)$; finaly, we also define $I_{8ij} = \boldsymbol{C}\colon\left(\boldsymbol{f}_i \otimes \boldsymbol{f}_j\right)$ with $i \neq j$. $\lambda_i, i = 1,2,3$ are the principal stretches; E_{ij} denote the components of the Green-Lagrange strain tensor $\boldsymbol{E}$. Subscript used in the expression of the E_{ij} refer either (i) to the cylindrical coordinate system (r,θ,z), (ii) to the global coordinate frame $(1,2,3)$ or (iii) to the locally orthogonal frame (f,s,n) where f is the fiber direction and s is the direction orthogonal to f but in the fiber plane. $I_k^*, k = 1,2,3$ are the invariants of the Green-Lagrange tensor $\boldsymbol{E}$. I_{4f}^* and I_{5f}^* are, respectively, $\boldsymbol{E}\colon\left(\boldsymbol{f}_i \otimes \boldsymbol{f}_i\right)$ and $\boldsymbol{E}^2\colon\left(\boldsymbol{f}_i \otimes \boldsymbol{f}_i\right)$.

7. Discussion

The number of constitutive equations is quite large, some interesting equations were listed in this chapter. A more exhaustive review can be found in [14]. Moreover, it exists other modelling approaches with a new class of elastic solids with implicit elasticity [135] that can also describe the strain limiting characteristics of soft tissues [136]. These theories are also elastic as they do not dissipate energies even if they are written in terms of strain rate and stress rate.

The question of the choice of the constitutive equation is a key point as it has large consequences on the simulations that can be performed. The links betwwen the initial material constants with the hyperelastic SEDF parameters are presented in this chapter for two classical models, but it is important to keep in mind that these relationship can only be used to initiate the identification optimization process.

Even today, for some applications, isotropic constitutive equations are abusely used to describe the mechanical behaviour of different soft tissues. In most of the cases, this simplifed models are misleading and inappropriate as most of soft tissues present a fibre structure that must be taken into account.

The use of anisotropic strain energy necessitates introducing fibre directions to model the mechanical properties of the soft tissue. Two ways of thinking exist, some consider that the fibre orientation should be physically motivated, i.e. that it represents the real orientation of fibres in the material, whereas some consider that the orientation of the fibre is one material parameter more. In this case the angle is just a mathematical parameter in a phenomenological model and the best fit is not necessarily obtained for the angle having a physical meaning.

In practise, the invariants I_2 and I_5 are often neglected. Their role in the strain energy is always difficult to identify [80]. Nevertheless, in some cases, their role can be very important [137]. A main difficulty relies on the fact that with only one mechanical test (for example only uniaxial test, or only equibiaxial test...), these invariants are linked to I_1 and I_4. That means that it is impossible to separate the contribution of each invariant. An important problem of the different constitutive equations is that it is difficult (or impossible) to separate the contribution of the matrix, the fibres and the interactions. The form of the equations does not present those parameters. Nevertheless, some authors try to separate the contribution of the isotropic and anisotropic parts [138]. To avoid such representations, physical approaches try to represent the repartition of fibres in space, but two difficulties must be considered, the knowledge of the distribution function of the fibres in space and the mechanical properties of a single fibre.

Nevertheless, the main difficulty is maybe not to have the best constitutive equation but to have experimental data in which one can be confident. One important problem is that the dispersion is often very large due to different patients, because of the age, the illness or other parameters. Another difficulty is that the definition of the boundary conditions is always very complicated and generates important errors on experimental data. As a consequence, one can wonder if the key point is to obtain the best fit for a very specific experimental database, or if the most important is to represent globally the mechanical behaviour keeping in mind the physics of the soft tissues. Anyway to correctly fit experimental data, it is crucial to have the maximum of different loading conditions to analyse the role of the different parameters of the constitutive equation. The equations are often implemented in finite element codes to describe any loading conditions. These conditions can be very far from uniaxial or biaxial loadings. In this case, it is important to choose a constitutive equation that can be fitted with few experimental data that do not simulate non-physical response for any loading. Generally, it is better to limit the number of invariants and

of material parameters. Moreover, the simplest functions are often the less risky as they cannot create non-physical responses even if their fitting is not the best. Another limitation is that, very few in vivo experimental data are available, they would be a benefit to the experimental fit [139].

8. Conclusion

It is difficult to compare two constitutive equations, the comparison depends on the studied soft tissues and the conclusions will strongly depend on the chosen experimental data. Nevertheless, some comparisons between anisotropic strain energies were realised in particular cases, see for example [54, 62, 66, 140, 141, 142].

This chapter presents only the basis of the hyperelasticity modelling, but soft tissues present a lot of other phenomena, that should be taken into account in the modelling according to the medical problem that is simulated, one can quote the activation of muscle (see chapter II of this book) or the viscoelasticity of the tissues (see chapter III of this book) [143, 9, 144, 145, 146] or the stress softening [12, 26] for example. Nevertheless, the hyperelasticity representation remains the starting point in a modelling and should be described as well as possible before introducing other phenomena.

References

[1] R.W. Ogden, Non-Linear elastic deformation, Dover, 1984

[2] S.C. Cowin, J.D. Humphrey, Cardiovascular soft tissue mechanics, Kluwer Academic Publisher, 2000

[3] G. A. Holzapfel, Nonlinear solid mechanics. A continuum approach for engineering, 2000. West Sussex, England: John Wiley & Sons, Ltd

[4] L.A. Taber, Nonlinear theory of elasticity, Word Scientific, 2004

[5] G.A. Holzapfel, R.W. Ogden, Mechanics of biological tissue, Springer, 2006.

[6] E. Marieb, K. Hoehn, Human Anatomy & Physiology., Pearson Education., 2010.

[7] J. D. Humphrey, Continuum biomechanics of soft biological tissues, Proc. R. Soc. Lond. A 459 (2003) 3–46.

[8] P. Kalita, R. Schaefer, Mechanical models of artery walls, Arch Comput Methods Eng 15 (2008) 1–36.

[9] J. E. Bischoff, E. M. Arruda, K. Grosh, A rheological network model for the continuum anisotropic and viscoelastic behavior of soft tissue, Biomech Model Mechanobiol 3 (2004) 56–65.

[10] T. P. Prevost, A. Balakrishnan, S. Suresh, S. Socrate, Biomechanics of brain tissue, Acta Biomater. 7 (2011) 83–95.

[11] E. Peña, P. Martins, T. Mascarenhasd, R. M. Natal Jorge, A. Ferreira, M. Doblaré, B. Calvo, Mechanical characterization of the softening behavior of human vaginal tissue, J. Mech. Behav. Biomed. 4 (2011) 275–283.

[12] E. Maher, A. Creane, C. Lally, D. J. Kelly, An anisotropic inelastic constitutive model to describe stress softening and permanent deformation in arterial tissue, J. Mech. Behav. Biomed. (2012) 9–19.

[13] J. Ohayon, A. M. Gharib, A. Garcia, J. Heroux, S. K. Yazdani, M. Malvé, P. Tracqui, M.-A. Martinez, M. Doblare, G. Finet, R. I. Pettigrew, Is arterial wall-strain stiffening an additional process responsible for atherosclerosis in coronary bifurcations?: an in vivo study based on dynamic CT and MRI, Am J Physiol Heart Circ Physiol. 301, (2011) H1097–106.

[14] G. Chagnon, M. Rebouah, D. Favier, Hyperelastic energy densities for soft biological tissues: a review., J. Elast. 120 (2015) 129–160.

[15] G. F. Smith, R. S. Rivlin, The anisotropic tensors, Quarterly of Applied Mathematics 15 (1957) 309–314.

[16] J. Boehler, A simple derivation of representations for non-polynomial constitutive equations in some cases of anisotropy, ZAMM - J. Appl. Math. Mech. 59 (1979) 157–167.

[17] A. J. M. Spencer, Theory of Invariants, Continuum Physics, C. Eringen Academic Press, 1971.

[18] G. A. Holzapfel, M. Stadler, T. C. Gasser, Changes in the mechanical environment of stenotic arteries during interactionwith stents: computational assessment of parametric stent design, J. Biomech Eng. 127 (2005) 166–180.

[19] J. L. Ericksen, R. S. Rivlin, Large elastic deformations of homogeneous anisotropic materials, Arch. Rational. Mech. Anal. 3 (1954) 281301.

[20] J. C. Criscione, A. S. Douglas, W. C. Hunter, Physically based strain invariants set for materials exhibiting transversely isotropic behavior, J. Mech. Phys. Solids 49 (2001) 871–891.

[21] M. Itskov, N. Aksel, A class of orthotropic and transversely isotropic hyperelastic constitutive models based on a polyconvex strain energy function, Int. J. Solids Struct. 41 (2004) 3833–3848.

[22] J. Murphy, Transversely isotropic biological, soft tissue must be modelled using both anisotropic invariants, Eur. J. Mech. A Solids 42 (2013) 90–96.

[23] G. Limbert, M. Taylor, On the constitutive modeling of biological soft connective tissues. a general theoretical framework and explicit forms of the tensors of elasticity for strongly anisotropic continuum fiber-reinforced composites at finite strain, Int. J. Solids Struct. 39 (2002) 2343–2358.

[24] J. Lu, X. Zhou, M. L. Raghavan, Computational method of inverse elastostatics for anisotropic hyperelastic solids, Int. J. Numer. Meth. Engng 69 (2007) 1239–1261.

[25] M. Kroon, G. A. Holzapfel, A new constitutive model for multilayered collagenous tissues, J. Biomech. 41 (2008) 2766–2771.

[26] E. Peña, J. A. Peña, M. Doblaré, On the Mullins effect and hysteresis of fibered biological materials: A comparison between continuous and discontinuous damage models, Int. J. Solids Struct. 46 (2009) 1727–1735.

[27] C. Sansour, On the physical assumptions underlying the volumetric-isochoric split and the case of anisotropy, Eur. J. Mech. A/Solids 27 (2008) 2839.

[28] J. Helfenstein, M. Jabareen, E. Mazza, S. Govindjee, On non-physical response in models for fiber-reinforced hyperelastic materials, Int. J. Solids Struct. 47 (2010) 2056–2061.

[29] M. Toungara, G. Chagnon, C. Geindreau, Numerical analysis of the wall stress in abdominal aortic aneurysm: influence of the material model near-incompressibility, J. Mech. Med. Biol. 12 (2012) 1–19.

[30] J. R. Walton, J. P. Wilber, Sufficient conditions for strong ellipticity for a class of anisotropic materials, Int. J. Non-linear Mech. 38 (2003) 441–455.

[31] H. C. Simpson, S. J. Spector, On copositive matrices and strong ellipticity for isotropic elastic materials, Arch. Rational Mech. Anal. 84 (1983) 55–68.
[32] L. Zee, E. Sternberg, Ordinary and strong ellipticity in the equilibrium theory of incompressible hyperelastic solids, Arch. Ration. Mech. Anal. 83 (1983) 53–90.
[33] J. Merodio, R. W. Ogden, Material instabilities in fiber-reinforced nonlinearly elastic solids under plane deformation., Arch. Mech. 54 (2002) 525–552.
[34] J. Merodio, R. W. Ogden, Instabilities and loss of ellipticity in fiber-reinforced compressible non-linearly elastic solids under plane deformation, Int. J. Solids Struct. 30 (2003) 4707–4727.
[35] O. Lopez-Pamies, M. I. Idiart, Fiber-reinforced hyperelastic solids: a realizable homogenization constitutive theory, J Eng Math 68 (2010) 57–83.
[36] A. Mielke, Necessary and sufficient conditions for polyconvexity of isotropic functions, J. Complex Analysis 12 (2005) 291–314.
[37] J. Schröder, P. Neff, Invariant formulation of hyperelastic transverse isotropy based on polyconvex free energy functions, Int. J. Solids Struct. 40 (2003) 401–445.
[38] J. Schröder, P. Neff, Poly-, quasi- and rank-one convexity in applied mechanics, CISM International Centre for Mechanical Sciences 516.
[39] J. M. Ball, Convexity conditions and existence theorems in non-linear elasticity, Archives for rational Mechanics and Analysis 63 (1977) 557–611.
[40] J. M. Ball, Constitutive equalities and existence theorems in elasticity, R.J. Knops (Ed.) Springer, Lecture Notes in Math. 316, 1977, Ch. Symposium on Non-well posed problems and logarithmic convexity.
[41] M. C. Boyce, E. M. Arruda, Constitutive models of rubber elasticity: a review, Rubber Chem. Technol. 73 (2000) 504–523.
[42] V. Vahapoglu, S. Karadeniz, Constitutive equations for isotropic rubber-like materials using phenomenological approach: a bibliography (1930-2003), Rubber Chem. Technol. 79 (2006) 489–499.
[43] H. Demiray, H. W. Weizsacker, K. Pascale, H. Erbay, A stress strain relation for a rat abdominal aorta, J. Biomech. 21 (1988) 369–374.
[44] M. Holmes, V. C. Mow, The non-linear characteristics of soft gels and hydrated connective tissues in ultrafiltration., J. Biomech. 23 (1990) 1145–1156.
[45] M. Nierenberger, Y. Rémond , S. Ahzi, A new multiscale model for the mechanical behavior of vein walls, J. Mech. Behav. Biomed. 23 (2013) 32–43.
[46] H. Chen, X. Zhao, X. Lu, G. Kassab, Nonlinear micromechanics of soft tissues, Int J. Non-Linear Mech. 56 (2013) 79–85.
[47] P. J. Flory, Statistical mechanics of chain molecules, New York, NY, 1969.
[48] A. Kloczkowski, Application of statistical mechanics to the analysis of various physicalproperties of elastomeric networks - a review, Polymer 43 (2002) 1503–1525.
[49] M. F. Beatty, An average-stretch full-network model for rubber elasticity., J. Elas. 70, (2004) 65–86.
[50] O. Kratky, G. Porod, Röntgenuntersuchungen gelöster fadenmoleküle, Recueil Trav. Chim. 68 (1949) 1106–1122.
[51] A. D. Freed, D. R. Einstein, I. Vesely, Invariant formulation for dispersed transverse isotropy in aortic heart valves, Biomechan. Model. Mechanobiol. 4 (2005) 100–117.
[52] Y. Lanir, Structure-strength relations in mammalian tendon, Biophys. 24 (1978) 541–554.
[53] J. Kastelic, I. Palley, E. Baer, A structural mechanical model for tendon crimping, J. Biomech. 13 (1980) 887.
[54] G. A. Holzapfel, T. C. Gasser, R. W. Ogden, A new constitutive framework for arterial wall mechanics and a comparative study of material models, J. Elast. 61 (2000) 1–48.
[55] S. Baek, R. L. Gleason, K. R. Rajagopal, J. D. Humphrey, Theory of small on large: potential utility in computations of fluid-solid interactions in arteries, Comput. Methods Appl. Mech. Engrg. 196 (2007) 3070–3078.
[56] I. Masson, P. Boutouyrie, S. Laurent, J. D. Humphrey, M. Zidi, Characterization of arterial wall mechanical behavior and stresses from human clinical data, J. Biomech. 41 (2008) 2618–2627.
[57] T. C. Gasser, G. A. Holzapfel, A rate-independent elastoplastic constitutive model for biological fiber-reinforcedcomposites at finite strains: continuum basis, algorithmic formulationand finite element implementation, Comput. Mech. 29 (2002) 340–360.
[58] X. Zhao, M. L. Raghavan, J. Lu, Identifying heterogeneous anisotropic properties in cerebral aneurysms: a point wise approach, Biomech. Model. Mechanobiol. 10 (2011) 177–189.
[59] P. Tong, Y. C. Fung, The stress-strain relationship for the skin, J. Biomech. 9 (1976) 649–657.
[60] Y. C. Fung, K. Fronek, P. Patitucci, Pseudoelasticity of arteries and the choice of its mathematical expression,

Am. Phys/ Soc. 237 (1979) H620–H631.
[61] C. J. Chuong, Y. C. Fung, Three-dimensional stress distribution in arteries, J. Biomech. Engrg 105 (3) (1983) 268–274.
[62] J. D. Humphrey, Mechanics of arterial wall: Review and directions, Critical Reviews in Biomed. Engr. 23 (1995) 1–162.
[63] J. M. Guccione, A. Salahieh, S. M. Moonly, J. Kortsmit, A. Wallace, M. B. Ratcliffe, Myosplint decreases wall stress without depressing function in the failing heart: a finite element model study, Ann. Thorac. Surg. 76 (2003) 1171–1180.
[64] R. N. Vaishnav, J. T. Young, D. J. Patel, Distribution of stresses and of strain-energy density through the wall thickness in a canine aortic segment., Circ. Res. 32 (1973) 577–583.
[65] K. Rajagopal, C. Bridges, K. R. Rajagopal, Towards an understanding of the mechanics underlying aortic dissection, Biomechan Model Mechanobiol 6 (2007) 345–359.
[66] J. D. Humphrey, Cardiovascular solid mechanics. Cells, Tissues and Organs, Springer, New York, 2002.
[67] M. P. Nash, P. J. Hunter, Computational mechanics of the heart: from tissue structure to ventricular function, J Elasticity 61 (2000) 113–141.
[68] J. P. Wilber, J. R. Walton, The convexity properties of a class of constitutive models for biological soft tissues, Math. Mech. Solids 7 (2002) 217–235.
[69] S. Federico, A. Grillo, S. Imatani, G. Giaquinta, W. Herzog, An energetic approach to the analysis of anisotropic hyperelastic materials, Int. J. Eng. Sci. 46 (2008) 164–181.
[70] R. S. Rivlin, D. W. Saunders, Large elastic deformations of isotropic materials - VII. Experiments on the deformation of rubber, Philos. Trans. R. Soc. A243 (1951) 251–288.
[71] M. Kaliske, A formulation of elasticity and viscoelasticity for fibre reinforced material at small and finite strains, Comput. Methods Appl. Mech. Engrg 185 (2000) 225–243.
[72] N. Triantafyllidis, R. C. Abeyaratne, Instability of a finitely deformed fiber-reinforced elastic material, J. Appl. Mech. 50 (1983) 149–156.
[73] M. Destrade, M. D. Gilchrist, D. A. Prikazchikov, G. Saccomandi, Surface instability of sheared soft tissues., J. Biomech. Eng. 130.
[74] X. Ning, Q. Zhu, Y. Lanir, S. S. Margulies, A transversely isotropic viscoelastic constitutive equation for brainstem undergoing finite deformation., J. Biomech. Eng. 128 (2006) 925–933.
[75] O. Rohrle, A. J. Pullan, Three-dimensional finite element modelling of muscle forces during mastication., J. Biomech. 40 (2007) 3363–3372.
[76] V. Alastrué, M. A. Martinez, M. Doblaré, A. Menzel, On the use of the bingham statistical distribution in microsphere-based constitutive models for arterial tissue, Mech. Res. Comm. 37 (2010) 700–706.
[77] L. W. Brown, L. M. Smith, A simple transversely isotropic hyperelastic constitutive model suitable for finite element analysis of fiber reinforced elastomers, J. Eng. Mater. Technol. 133 (2011) 1–13.
[78] M. Ruter, E. Stein, Analysis, finite element computation and error estimation in transversely isotropic nearly incompressible finite elasticity, Comput. Methods Appl. Mech. Engrg. 190 (2000) 519–541.
[79] C. O. Horgan, G. Saccomandi, A new constitutive theory for fiber-reinforced incompressible nonlinearly elastic solids, J. Mech. Phys. Solids 53 (2005) 1985–2015.
[80] J. D. Humphrey, R. K. Strumph, F. C. P. Yin, Determination of a constitutive relation for passive myocardium. I. a new functional form, ASME J. Biomech. Engrg. 15 (1990) 1413–1418.
[81] S. Jemiolo, J. J. Telega, Transversely isotropic materials undergoing large deformations and application to modelling soft tissues, Mech. Res. Commun. 28 (2001) 397–404.
[82] C. A. Basciano, C. Kleinstreuer, Invariant-based anisotropic constitutive models of the healthy and aneurysmal abdominal aortic wall, J. Biomech. Eng. ASME 131 (2009) 1–11.
[83] J. D. Humphrey, F. C. P. Yin, On constitutive relations and finite deformations of passive cardiac tissue: I. a pseudo strain-energy approach, ASME J. Biomech. Engrg. 109 (1987) 298–304.
[84] G. A. Holzapfel, G. Sommer, C. T. Gasser, P. Regitnig, Determination of the layer-specific mechanical properties of human coronary arteries with non-atherosclerotic intimal thickening, and related constitutive modelling., Am. J. Physiol. Heart Circ. Physiol. 289 (2005) H2048–2058.
[85] J. A. Weiss, B. N. Maker, S. Govindjee, Finite implementation of incompressible, transversely isotropic hyperelasticity, Comput. Methods Appl. Mech. Engrg. 135 (1996) 107–128.
[86] P. Ciarletta, I. Izzo, S. Micera, F. Tendick, Stiffening by fiber reinforcement in soft materials: A hyperelastic theory at large strains and its application, J. Mech. Biomed. Mater. 4 (2011) 1359–1368.
[87] P. M. Pinsky, D. van der Heide, D. Chernyak, Computational modeling of mechanical anisotropy in the cornea and sclera, J Cataract Refract Surg 31 (2005) 136–145.

[88] A. N. Natali, P. G. Pavan, E. L. Carniel, C. Dorow, A transversally isotropic elasto-damage constitutive model for the periodontal ligament, Comput. Method Biomech 6 (2003) 329–336.
[89] E. Peña, B. Calvo, M. A. Martinez, P. Martins, T. Mascarenhas, R. M. N. Jorge, A. Ferreira, M. Doblaré, Experimental study and constitutive modeling of the viscoelastic mechanical properties of the human prolapsed vaginal tissue, Biomech. Model. Mechanobiol. 9 (2010) 35–44.
[90] T. C. Gasser, R. W. Ogden, G. A. Holzapfel, Hyperelastic modelling of arterial layers with distributed collagen fibre orientations, J. R. Soc. Interface 3 (2006) 15–35.
[91] K. May-Newman, C. Lam, F. C. P. Yin, A hyperelastic constitutive law for aortic valve tissue, J. Biomech. Eng. 131 (2009) 1–7.
[92] E. Peña, Prediction of the softening and damage effects with permanent set in fibrous biological materials, J. Mech. Phys. Solids 59 (2011) 1808–1822.
[93] I. Masson, C. Fassot, M. Zidi, Finite dynamic deformations of a hyperelastic, anisotropic, incompressible and prestressed tube. Applications to in vivo arteries, Eur. J. Mech. A/Solids 29 (2010) 523–529.
[94] A. Valencia, F. Baeza, Numerical simulation of fluidstructure interaction in stenotic arteries considering two layer nonlinear anisotropic structural model, Int. Com. Heat Mass Transf. 36 (2009) 137–142.
[95] M. Qian, D. M. Wells, A. Jones, A. Becker, Finite element modelling of cell wall properties for onion epidermis using a fibre-reinforced hyperelastic model, J. Struct. Biol. 172 (2010) 300–304.
[96] G. Chagnon, V. Gaudin, D. Favier, L. Orgeas, P. Cinquin, An osmotically inflatable seal to treat endoleaks of type 1, J. Mech. Med. Biol. 12 (2012) 1250070.
[97] A. Pandolfi, F. Maganiello, A model for the human cornea: constitutive formulation and numerical analysis., Biomechan. Model. Mechanobiol. 5 (2006) 237–246.
[98] T. Kloppel, W. A. Wall, A novel two-layer, coupled finite element approach for modeling the nonlinear elastic and viscoelastic behavior of human erythrocytes, Biomech Model Mechanobiol 10 (2011) 445–459.
[99] V. Prot, R. Haaverstad, B. Skallerud, Finite element analysis of the mitral apparatus: annulus shape effect and chordal force distribution, Biomech. Model. Mechanobiol. 8 (2009) 43–55.
[100] O. Trabelsi, A. Pérez del Palomar, J. L. Lopez-Villalobos, A. Ginel, M. Doblaré, Experimental characterization and constitutive modeling of the mechanical behavior of the human trachea, Med. Eng. Phys. 32 (2010) 76–82.
[101] M. Malvè, A. Pérez del Palomar, O. Trabelsi, J. L. Lopez-Villalobos, A. Ginel, M. Doblaré, Modeling of the fluid structure interaction of a human trachea under different ventilation conditions, Int. Comm. Heat Mass Transf. 38 (2011) 10–15.
[102] E. Lanchares, B. Calvo, J. A. Cristobal, M. Doblaré, Finite element simulation of arcuates for astigmatism correction, J. Biomech. 41 (2008) 797–805.
[103] T. D. Nguyen, B. L. Boyce, An inverse finite element method for determining the anisotropic properties of the cornea, Biomech. Model. Mechanobiol. 10 (2011) 323–337.
[104] I. Karsaj, C. Sansour, J. Soric, The modelling of fibre reorientation in soft tissue, Biomech. Model. Mechanobiol. 8 (2009) 359–370.
[105] B. Hernandez, E. Peña, G. Pascual, M. Rodriguez, B. Calvo, M. Doblaré, J. M. Bellon, Mechanical and histological characterization of the abdominal muscle. a previous step to modelling hernia surgery, J. Mech. Biomed. Mater. 4 (2011) 392–404.
[106] A. L. Dorfmann, W. A. Woods Jr., B. A. Trimmer, Muscle performance in a soft-bodied terrestrial crawler: constitutive modeling of strain-rate dependency, J. R. Soc., Interface 5 (2008) 349–362.
[107] G. Limbert, J. Middleton, A transversely isotropic viscohyperelastic material application to the modeling of biolgical soft connective tissues, Int. J. Solids Struct. 41 (2004) 4237–4260.
[108] B. Calvo, E. Peña, P. Martins, T. Mascarenhas, M. Doblaré, R. M. Natal Jorge, A. Ferreira, On modelling damage process in vaginal tissue, J. Biomech. 42 (2009) 642–651.
[109] R. W. Ogden, G. Saccomandi, Introducing mesoscopic information into constitutive equations for arterial walls, Biomechan Model Mechanobiol 6 (2007) 333344.
[110] B. Markert, W. Ehlers, N. Karajan, A general polyconvex strain-energy function for fiber-reinforced materials, Proc. Appl. Math. Mech. 5 (2005) 245–246.
[111] H. Demirkoparan, T. Pence, Swelling of an internally pressurized nonlinearly elastic tube with fiber reinforcing, Int. J. Solids Struct. 44 (2007) 4009–4029.
[112] H. Demirkoparan, T. J. P. ans A. Wineman, On dissolution and reassembly of filamentary reinforcing networks in hyperelastic materials, Proc. R. Soc. A 465 (2009) 867–894.
[113] D. Lurding, Y. Basar, U. Hanskotter, Application of transversely isotropic materials to multi-layer shell elements undergoing finite rotations and large strains, Int. J. Solids Struct. 38 (2001) 9493–9503.
[114] S. Reese, T. Raible, P. Wriggers, Finite element modelling of orthotropic material behaviour in pneumatic

membranes, Int. J. Solids Struct. 38 (2001) 9525–9544.
[115] G.A. Holzapfel and R.W. Ogden, Constitutive modelling of passive myocardium: a structurally based framework for material characterization. Phil. Trans. R. Soc. A. 367 (2009) 3445–75.
[116] N. T. Hollingsworth, D. R. Wagner, Modeling shear behavior of the annulus fibrosus, J. Mech. Biomed. Mater. 4 (2011) 1103–1114.
[117] A. J. M. Spencer, Continuum theory of the mechanics of fibre-reinforced composites, Springer, New-York, 1984.
[118] M. Itskov, A. E. Ehret, D. Mavrilas, A polyconvex anisotropic strain energy function for soft collagenous tissues, Biomech Model Mechanbiol 5 (2006) 1726.
[119] A. E. Ehret, M. Itskov, A polyconvex hyperelastic model for fiber-reinforced materials in application to soft tissues, J. Mater. Sci. 42 (2007) 8853–8863.
[120] A. N. Natali, E. L. Carniel, H. Gregersen, Biomechanical behaviour of oesophageal tissues: Material and structural configuration, experimental data and constitutive analysis, Med. Eng. & Phys. 31 (2009) 1056–1062.
[121] N. L. Nerurkar, R. L. Mauck, D. M. Elliott, Modeling interlamellar interactions in angle-ply biologic laminates for annulus fibrosus tissue engineering, Biomech Model Mechan 10 (2011) 973–984.
[122] S. Göktepe, S. N. S. Acharya, J. Wong, E. Kuhl, Computational modeling of passive myocardium, Int. J. Numer. Meth. Biomed. Engng. 27 (2011) 112.
[123] X. Peng, Z. Guo, T. Du, W. R. Yu, A simple anisotropic hyperelastic constitutive model for textile fabrics with application to forming simulation, Composites: Part B 52 (2013) 275–281.
[124] M. Rebouah, G. Chagnon, Permanent set and stress softening constitutive equation applied to rubber like materials and soft tissues, Acta Mech. 225, (2014) 1685–1698.
[125] X. Q. Peng, Z. Y. Guo, B. Roman, An anisotropic hyperelastic constitutive model with fiber-matrix shear interaction for the human annulus fibrosus, J. Appl. Mech. Trans ASME 73 (2006) 815–824.
[126] Z. Y. Guo, X. Q. Peng, B. Moran, Large deformation response of a hyperelastic fibre reinforced composite: Theoretical model and numerical validation, Composites Part A 38 (2007) 18421851.
[127] Z. Y. Guo, X. Q. Peng, B. Moran, Mechanical response of neo-hookean fiber reinforced incompressible nonlinearly elastic solids, Int. J. Solids Struct. 44 (2007) 1949–1969.
[128] Z. Y. Guo, X. Q. Peng, B. Moran, A composites-based hyperelastic constitutive model for soft tissue with application to the human annulus fibrosus, J. Mech. Phys. Solids 54 (2006) 1952–1971.
[129] F. C. Caner, Z. Guo, B. Moran, Z. P. Bazant, I. Carol, Hyperelastic anisotropic microplane constitutive model for annulus fibrosus, Transactions of the ASME 129 (2007) 1–10.
[130] J. F. Rodriguez, C. Ruiz, M. Doblaré, G. A. Holzapfel, Mechanical stresses in abdominal aortic aneurysms: influence of diameter, asymmetry, and material anisotropy., ASME J. Biomech. Eng. 130.
[131] J. B. Caulfield, J. S. Janicki, Structure and function of myocardial fibrillar collagen. Technology and Health Care., IOS Press, 5 (1997) 95–113.
[132] C. Bourdarias, S. Gerbi, J. Ohayon, A pseudo active kinematic constraint for a biological living soft tissue: An effect of the collagen network. Math. Comput. Model., 49 (2009) 2170–2181.
[133] C. Bourdarias, S. Gerbi, J. Ohayon, A three dimensional finite element method for biological active soft tissue -Formulation in cylindrical polar coordinates. Mathematical Modelling and Numerical Analysis. M2AN, 37 (2003) :725–739.
[134] G. A. Holzapfel, Nonlinear Solid Mechanics, A Continuum Approach For Engineering (2001), John Wiley & Sons Ltd.
[135] K. Rajagopal, On implicit constitutive theories, Appl. Math. 48 (2003) 279–319.
[136] A. D. Freed, D. R. Einstein, An implicit elastic theory for lung parenchyma, Int. J. Eng. Sci. 62 (2013) 31–47.
[137] Y. Feng, R. J. Okamoto, R. Namani, G. M. Genin, P. V. Bayly, Measurements of mechanical anisotropy in brain tissue and implications for transversely isotropic material models of white matter, J. Mech. Beh. Biomed. Mater. 23 (2013) 117–132.
[138] N. Harb, N. Labed, M. Domaszewski, F. Peyraut, A new parameter identification method of soft biological tissue combining genetic algorithm with analytical optimization, Comput. Methods Appl. Mech. Engrg. 200 (2011) 208–215.
[139] C. A. J. Schulze-Bauer, G. A. Holzapfel, Determination of constitutive equations for human arteries from clinicaldata, J. Biomechanics 36 (2003) 165–169.
[140] M. Carboni, G. W. Desch, H. W. Weizsacker, Passive mechanical properties of porcine left circumflex artery and its mathematical description, Med. Eng. Phys. 29 (2007) 8–16.
[141] R. P. Vito, S. A. Dixon, Blood vessel constitutive models 1995-2002, Annu. Rev. Biomed. Eng. 5 (2003) 413–439.
[142] B. Galle, H. Ouyang, R. Shi, E. Nauman, A transversely isotropic constitutive model of excised guinea pig

spinal cord white matter, J. Biomech. 43 (2010) 2839–2843.
[143] G. A. Holzapfel, T. C. Gasser, M. Stadler, A structural model for the viscoelastic behavior of arterial walls: continuum formulation and finite element analysis, Eur. J. Mech. A/Solids 21 (2002) 441–463.
[144] V. Quaglini, P. Vena, R. Contro, A discrete-time approach to the formulation of constitutive models for viscoelastic soft tissues, Biomech Model Mechan 3 (2004) 85–97.
[145] H. W. Haslach, Nonlinear viscoelastic, thermodynamically consistent, models for biological soft tissue, Biomech. Model. Mechanobio. 3 (2005) 172–189.
[146] G. Limbert, J. Middleton, A constitutive model of the posterior cruciate ligament, Med. Eng. Phys. 28 (2006) 99–113.